RSC Advances

PAPER

View Article Online
View Journal | View Issue

Cite this: *RSC Adv.*, 2020, **10**, 34254

Microencapsulated UV filter@ZIF-8 based sunscreens for broad spectrum UV protection†

Anu Sharma, [ab] Abhishek Kumar, [b] Changning Li, [b] Rakesh Kumar Sharma*[a] and Mark T. Swihart *[bc]

Sunscreens play a vital role in protecting human skin from photodamage upon UV exposure, but their effectiveness is limited by degradation and phototoxicity. Photoactivation of UV filters in sunscreen can generate reactive oxygen species, with accompanying cytotoxicity. Herein, we report stable, safe, fluorescent, and long-lasting sunscreens produced by microencapsulation of organic UV filters octylmethoxycinnamate (OMC) and butyl-methoxydibenzoylmethane (BMDM), alone and together, into a microporous zeolitic imidazole framework (ZIF-8). The visibly transparent OMC + BMDM@ZIF-8 sunscreens displayed complete broad-spectrum photoprotection against UV light even after 24 hours. Photostability testing of the sunscreens demonstrated the photo-protective nature of microporous ZIF-8 for stabilizing these UV filters. The sun protection factor (SPF) values for lotions containing 10% (w/w) OMC@ZIF-8, BMDM@ZIF-8 and OMC + BMDM@ZIF-8 sunscreens decreased from 29.8 to 26.0, 32.5 to 26.4, and 62.1 to 53.0, respectively, upon 24 hours of intense UV exposure. No release of the UV filters from the encapsulated formulations was observed. The ZIF-8 particles are too large to be transported across the stratum corneum. Thus, our findings suggest that zeolitic framework-encapsulated sunscreens could provide prolonged UV-protection efficacy and ultra-high SPF with reduced potential for degradation, phototoxicity, and transport across the skin.

Received 3rd July 2020
Accepted 4th September 2020

DOI: 10.1039/d0ra05828a

rsc.li/rsc-advances

Introduction

Exposure to sunlight plays vital roles in human physiology, including triggering the production of vitamin D, the "sunshine vitamin". The many positive effects of solar exposure include protecting us from some types of cancer and inflammation, enhancing activity of mitochondria to provide energy for daily activities, improving brain function, and lowering blood pressure. Exposure to ultraviolet (UVA/UVB) radiation from sunlight in the right dose can cure and prevent rickets and stimulate blood circulation.[1,2] However, overexposure to UV light can induce detrimental effects on human skin such as photoaging, oxidative stress, photocarcinogenesis, RNA and DNA damage, erythema formation, and immunosuppression.[3,4] UV filters and sunscreen formulations have been engineered to prevent overexposure. Sunscreens are broadly classified as chemical sunscreens (organic sunscreens) and physical sunscreens (inorganic sunscreens). These active materials reduce UV damage by absorbing or scattering UV rays before they interact with human skin.[5] Physical sunscreens like ZnO and TiO_2 can reduce UV damage through scattering, reflection, and diffraction of UV rays, as well as by absorption of UV rays, but may result in discomfort and degradation of other components. Photocatalytic activity of TiO_2 can degrade biomolecules such as RNA and membrane proteins. Chemical sunscreens such as octylmethoxycinnamate (OMC) and butylmethoxydibenzoylmethane (BMDM) minimize UV damage through absorption. However, their lifetime is short due to photodegradation, and they can also be phototoxic.[6,7] Moreover, they can cause inflammation of the skin by allergic reactions and can even mimic the estrogen hormone, which is a serious concern.[8,9]

Hence, the primary concerns associated with existing sunscreens include limited photostability, negative health effects due to generation of reactive oxygen species (ROS) under solar irradiation, loss of effectiveness by simple removal from the skin, and penetration through the skin. UV filters such as OMC (UVB filter) and BMDM (UVA filter) can bioaccumulate in blood and be metabolized in the body. They have been detected in human blood plasma, urine, and breast milk.[10,11] ROS produced by these filters upon photodegradation can be more harmful to skin cells than the UV filters themselves. These ROS not only penetrate into the skin but also damage DNA and

[a]*Department of Chemistry, University of Delhi, India. E-mail: sharmark101@yahoo.com*

[b]*Department of Chemical and Biological Engineering, University at Buffalo (SUNY), USA. E-mail: swihart@buffalo.edu*

[c]*RENEW Institute, University at Buffalo (SUNY), USA*

† Electronic supplementary information (ESI) available: BET adsorption isotherms of ZIF-8, OMC@ZIF-8, BMDM@ZIF-8 and OMC + BMDM@ZIF-8; calibration curves of OMC and BMDM absorbance *vs.* concentration; degradation data for UV filters alone; and pore parameters of ZIF-8 and microencapsulated filters. See DOI: 10.1039/d0ra05828a

degrade proteins and nucleic acids, leading to structural changes that directly affect their biological function.[12] Thus, key limitations of current organic sunscreens, including their degradation upon extended solar irradiation and their potential for generation of ROS, are still not resolved.[13,14] Moreover, sunscreens should be formulated to remain on the surface of the skin, to avoid the harmful effects caused by the penetration of these UV filters into the skin. To enhance their stability and to minimize their transcutaneous absorption, one can encapsulate them in suitable matrices, such as lipids, polymers, nanoparticles, or other structures.

Several methods have been reported for physical or covalent attachment onto or encapsulation into a biocompatible polymer matrix to avoid exposure of skin cells to ROS produced by organic sunscreens. However, the porosity and degradability of some encapsulating materials allow the UV filters or ROS generated by them to leach out. To avoid this, the structural characteristics of the encapsulating material should minimize diffusion of ROS, increase dissipation of energy, immobilize the encapsulated component, and thereby enhance the stability of the sunscreen. Encapsulation of UV filters into nanoparticles may also overcome solubility limits and increase the maximum quantity that can be incorporated into a lotion, reduce the use of other chemicals, and provide photostabilization.[2,15,16] Nanoscale ZIF-8, a metal–organic framework synthesized from a zinc salt and the organic linker 2-methylimidazole is a potential candidate for encapsulation of guest molecules and has shown promise for applications in drug delivery, sensing, adsorption, and separation. It has a high surface area with a robust structure, is biocompatible, and features a pore size and large pore volume that make it a suitable candidate for biomedical applications.[7]

Here, we demonstrate the microencapsulation of OMC and BMDM alone and in combination within microparticles of ZIF-8 to minimize the harmful effects of UV filters by eliminating their direct contact with skin and their potential for transcutaneous transport (Fig. 1). As illustrated schematically in Fig. 1(b) these molecules easily fit within the cage-like structures in the sodalite-type lattice of ZIF-8, but cannot fit through the ~3 Å pores connecting the cages. This allows ZIF-8 to irreversibly encapsulate the organic sunscreens in these nanocapsules. The OMC@ZIF-8, BMDM@ZIF-8, and OMC + BMDM@ZIF-8 nanocapsules were characterized by powder X-ray diffraction (XRD), Scanning Electron Microscopy (SEM), Transmission Electron Microscopy (TEM), Fourier transform infrared spectroscopy (FTIR), ultraviolet-visible spectroscopy (UV-vis), and Brunauer–Emmett–Teller (BET) analysis of nitrogen physisorption. Results of these analyses show that nanocapsules loaded with sunscreens have excellent photostability (≥85%) upon UV exposure for 24 hours, maintaining ultra-high SPF with no leaching of the encapsulated UV filters. In short, these sunscreens are safe, long-lasting, and provide a new direction in the field of UV-protective cosmetics.

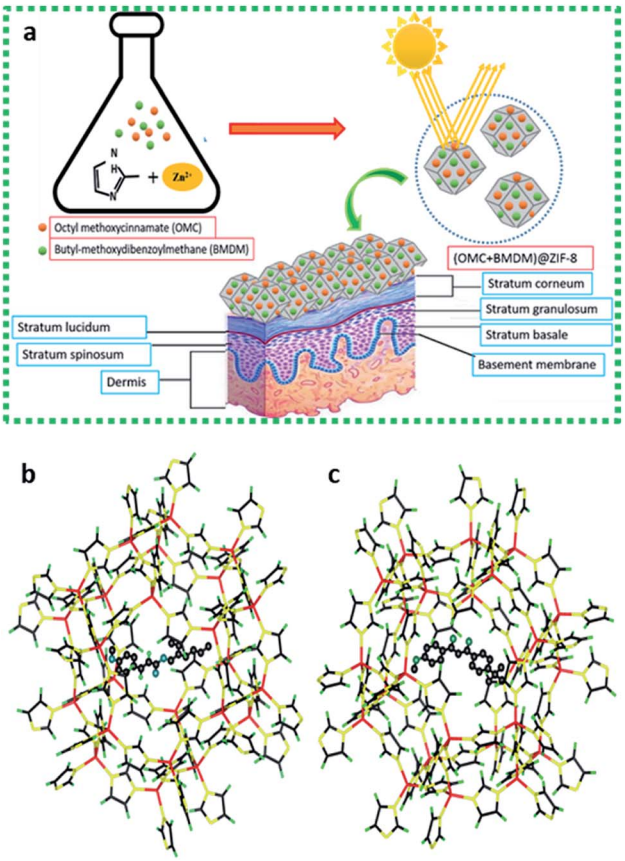

Fig. 1 (a) Schematic illustration of the *in situ* microencapsulation of OMC and BMDM in microporous zeolitic imidazole framework and their function as a sunscreen. Microencapsulation of UV filters reduces leaching, degradation and transdermal penetration upon UV exposure; and (b and c) molecular models illustrating the encapsulation of (b) OMC and (c) BMDM within single cage of the ZIF-8 structure. In each case, the encapsulated molecule is shown with balls representing the atoms, while only bonds are shown for the ZIF-8 cage.

Results and discussion

The UV-vis absorption spectra of ethanolic dispersions of ZIF-8 alone, the UV filters alone, and the UV filter-containing ZIF-8 nanocapsules were recorded over the range of 250 nm to 600 nm, at equal concentrations of UV filters, as shown in Fig. 2(a). The peak at 228 nm in ZIF-8 is due to the n–π* transition and confirms the presence of the imidazole ligand.[17] Free OMC and BMDM showed their characteristic peaks at 310 nm and 358 nm, respectively. The presence of peaks at 310 nm and 358 nm indicates the successful encapsulation of OMC and BMDM in ZIF-8 to form OMC@ZIF-8 and BMDM@ZIF-8 nanocapsules, respectively. The observation of both peaks in OMC + BMDM@ZIF-8 nanocapsules confirms the presence of both UV filters within it. Microencapsulation of UV filters into ZIF-8 shows a synergistic enhancement of absorbance because of strong chemical interactions of UV filters with the ZIF-8. The cages of ZIF-8 may provide a hydrophobic environment and may confine molecular motions to enhance absorption. The UV absorbance of OMC@ZIF-8 and BMDM@ZIF-8 nanocapsules is found to be 5.2 and 5.1 times greater than the individual OMC, and BMDM dispersed or dissolved in ethanol at the same concentration, while in OMC + BMDM@ZIF-8, the increase is 4.7 (for OMC) and 5.9 (for BMDM) as shown in Fig. 2(a). The

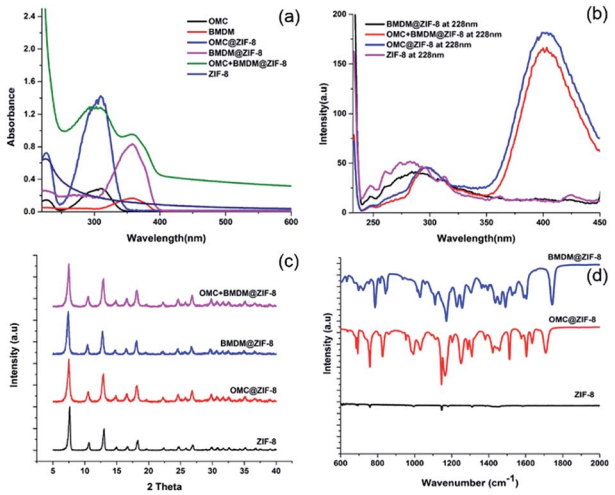

Fig. 2 (a) UV-vis spectra of ethanolic solutions of void ZIF-8, OMC@ZIF-8, BMDM@ZIF-8 and OMC + BMDB@ZIF-8. For each OMC-containing sample the OMC concentration was 5 μg mL^{-1}, and for each BMDM-containing sample, the BMDM concentration was 5 μg mL^{-1}. (b) Fluorescence spectra under 228 nm excitation (c) powder XRD patterns and (d) FTIR spectra of ZIF-8, OMC@ZIF-8, and BMDM@ZIF-8 nanocapsules.

inner cavities of ZIF-8 can also provide a hydrophobic environment for the microencapsulation of UV filters, overcoming their solubility limits in carrier lotions. The nanocapsules can scatter the incident UV radiation because of their overall size comparable to the wavelength of UV radiation. Therefore, the UV filter-loaded nanocapsules could show excellent UV photoprotective performance.

The fluorescence spectra of ZIF-8, OMC@ZIF-8, BMDM@ZIF-8, and OMC + BMDM@ZIF-8 nanocapsules were acquired under excitation at 228 nm as shown in Fig. 2(b). The ethanolic dispersions of nanocapsules showed significant fluorescence at UV and visible wavelengths. The fluorescence intensity of OMC@ZIF-8 and OMC + BMDM@ZIF-8 exceeded that of ZIF-8 because ZIF-8 acts as an energy donor and OMC acts as an acceptor that then emits at visible wavelengths near 400 nm. However, in the case of BMDM@ZIF-8, the fluorescence of ZIF-8 was quenched somewhat but no emission from BMDM was observed. Visible fluorescence from OMC can be of great value in studies of the fate and transport of these sunscreens, as it provides an easy means of tracking them, for example, in assays of skin penetration or removal from the skin.

The crystal structures of the ZIF-8 and ZIF-8 encapsulated UV filters were characterized by powder X-ray diffraction (XRD), as shown in the Fig. 2(c). The void ZIF-8 showed the expected diffraction peaks at 7.61°, 10.66°, 12.97°, 14.95°, 16.69° and 18.33°, which correspond to (011), (002), (112), (022), (013) and (222) lattice planes of ZIF-8, respectively.[18] OMC and BMDM are amorphous materials and hence do not have any characteristic diffraction peaks. Thus, the XRD patterns of ZIF-8 and UV filter-loaded ZIF-8 are the same. UV filter encapsulation does not disrupt the ZIF-8 crystal structure.

The Fourier Transform Infrared (FT-IR) spectra of void ZIF-8 and OMC@ZIF-8, and BMDM@ZIF-8 nanocapsules are depicted in Fig. 2(d). The broad peak between 1395 and 1500 cm^{-1} is attributed to imidazole ring stretching vibrations. The absorption peak from 1089 to 1179 cm^{-1} is due to C–H bending vibrations, and the peak around 1387 cm^{-1} represents C–C bonding. The absorption peaks at 1586 cm^{-1} and 421 cm^{-1} are due to the stretching modes of C=N and N–Zn, respectively. Observation of these groups confirms the presence of the imidazole ring.[19] In comparison to the void ZIF-8, the encapsulated UV filters have additional absorption peaks. The absorption at 1250 cm^{-1} and 1750 cm^{-1} can be attributed to C–O stretching vibrations of ester bonds present in OMC and BMDM.

The size and morphology of void ZIF-8 and encapsulated OMC@ZIF-8, BMDM@ZIF-8, and OMC + BMDM@ZIF-8 nanocapsules were characterized by Transmission Electron Microscopy (TEM), and the results are shown in Fig. 3. All the nanocapsules (ZIF-8, OMC@ZIF-8, BMDM@ZIF-8, and OMC + BMDM@ZIF-8) formed have the same rhombic dodecahedral morphology and uniform size near 200 nm. Encapsulation of the UV filters does not affect the morphology or size of ZIF-8. The size of nanocapsules plays an important role in the transdermal permeation. Prior reports have shown that nanocapsules with characteristic diameters ≥200 nm show minimal transdermal permeation. They can either migrate along/fill the hair follicle canals or can penetrate the stratum corneum but are not able to penetrate viable epidermis.[20] So, the developed nanocapsules reduce the potential for transdermal penetration of the UV filters.

Surface area and pore volume of the ZIF-8 and UV-filter loaded ZIF-8 were characterized by nitrogen physisorption

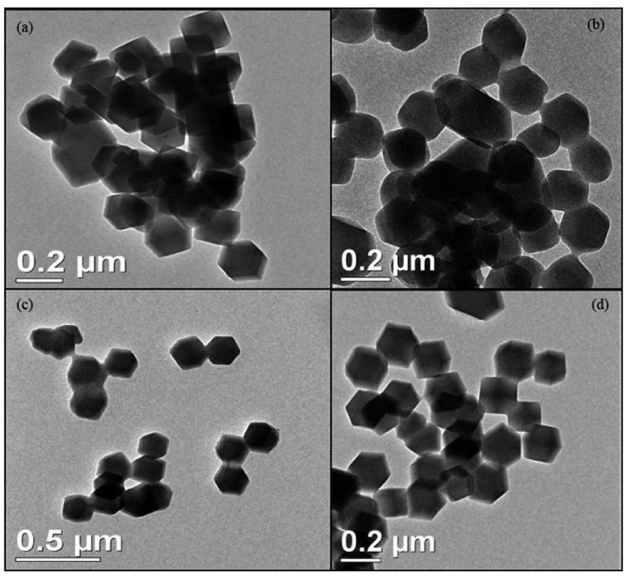

Fig. 3 Transmission Electron Microscopy (TEM) images of (a) ZIF-8, (b) OMC@ZIF-8, (c) BMDM@ZIF-8, and (d) OMC + BMDM@ZIF-8 showing their rhombic dodecahedron morphology with an average diameter of 200–205 nm.

(BET analysis). According to IUPAC nomenclature, the void ZIF-8 and the UV-filter loaded ZIF-8 nanocapsules show type I adsorption isotherms (Fig. S1†) and are microporous materials. The void ZIF-8, OMC@ZIF-8, BMDM@ZIF-8, and OMC + BMDM@ZIF-8 nanocapsules showed average pore diameters of 2.74 nm, 2.72 nm, 2.73 nm, and 2.72 nm, respectively. The average pore diameter remains almost the same in void ZIF-8 and microencapsulated ZIF-8 nanocapsules, indicating the UV filters are microencapsulated and not hosted within the pores of ZIF-8. The surface area and pore volume of void ZIF-8 by the BET method is 892 $m^2\ g^{-1}$ and 0.612 $cm^3\ g^{-1}$, which is higher than the UV-filter loaded ZIF-8 nanocapsules, as shown in Table ST1.† This decrease in specific surface area is consistent with the increased mass associated with UV filter encapsulation, which adds mass but not surface area. The larger effect for OMC compared to BMDM on the nitrogen uptake may indicate that the flexible portion of the OMC molecule is entering the pores of ZIF-8, blocking some pores, while the main rigid part of the molecule remains in the cage of the zeolitic structure.

To calculate the encapsulation efficiency of OMC and BMDM, calibration curves were constructed for solutions in ethanol at five different known concentrations, as shown in Fig. S2.† The initial concentration (0.125 g) of UV filters was considered as 100% encapsulation. Then UV-visible spectra were recorded for all nanocapsules and the supernatant from the synthesis, and encapsulated amounts were determined using calibration curves. The amount of entrapped OMC/BMDM into the nanocapsules was found to be 80%, 90%, and 92% of the amount added during synthesis for OMC@ZIF-8, BMDM@ZIF-8, and OMC + BMDM@ZIF-8, respectively. The storage stability of nanocapsules was assessed by TEM, XRD, and UV-vis spectroscopy, which showed that the nanocapsules are stable during 40 days of storage at ~25 °C. Thus, these nanocapsules need not be stored in the refrigerator.

As a carrier cream for these nanocapsules, Aveeno body lotion was chosen because its ingredients do not contain UV blocking chemicals. So, we can easily explore the effect of UV-filter loaded nanocapsules by blending them with the Aveeno body lotion. Absorbance spectra of the pure cream and the cream with UV-filter loaded nanocapsules are shown in Fig. 4(a). Pure cream alone has minimal UV absorbance. In UV-vis spectra, OMC@ZIF-8- and BMDM@ZIF-8-loaded sunscreens show absorbance at 310 nm and 358 nm, indicating the presence of nanocapsules. The OMC + BMDM@ZIF-8 based sunscreen showed absorbance at both 310 nm and 358 nm, reflecting the presence of both the UV filters loaded in the nanocapsules.

The photostability limitation of organic UV-filters is a key barrier to developing more effective long-lasting sunscreens. The concern with the UV filters OMC and BMDM is that they can degrade and generate free radicals upon extended UV exposure, and their sunscreen performance can be hindered.[2,15,16] The percentage degradation of 0.08% OMC and 0.09% BMDM mixed with Aveeno cream was found to be 53.5% and 61.6% after 24 hours of UV light irradiation, as shown in Fig. S3.† As shown here, encapsulating the UV filters into ZIF-8 reduced their degradation. Formulations containing 0.1% of each OMC@ZIF-8, BMDM@ZIF-8, and OMC + BMDM@ZIF-8 sunscreens showed photostability of 81.6%, 81.7%, and 94.9% respectively after 24 hours UV exposure (Fig. 4(b)). The OMC + BMDM@ZIF-8 sunscreen showed higher photostability than OMC@ZIF-8 and BMDM@ZIF-8 sunscreens.

For the determination of changes in structure, size, and morphology of nanocapsules upon UV irradiation, XRD and SEM analysis was performed. The XRD spectra were recorded for 4 sunscreen-loaded glass slides at 0 h, 4 h, and 24 h. No changes in the peak intensities or positions were observed after irradiating the slides for 4 h and 24 h. This suggests no distortion or collapse of nanocapsules occurred under UV exposure (Fig. 5(a)). In short, the stability of the structure clearly indicates the photostable nature of ZIF-8. SEM images shown in Fig. 5(b) were also taken at 0 h, and 24 h for the OMC + BMDM@ZIF-8 sunscreen coated glass slide. No changes in the morphology were observed before and after UV exposure. The photostability of OMC and BMDM were clearly enhanced by microencapsulation in ZIF-8.

The SPF value of 10% OMC@ZIF-8, BMDM@ZIF-8, and OMC + BMDM@ZIF-8 sunscreens decreased from 29.7 to 25.8, 32.4 to

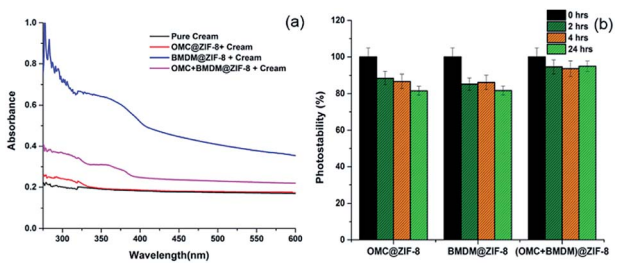

Fig. 4 (a) UV-vis spectra of pure cream (Aveeno body lotion) and OMC@ZIF-8, BMDM@ZIF-8, and OMC + BMDM@ZIF-8 nanocapsules after mixing with cream (b) photostability of void ZIF-8 and OMC@ZIF-8, BMDM@ZIF-8, and OMC + BMDM@ZIF-8 after 0, 2, 4 and 24 hours.

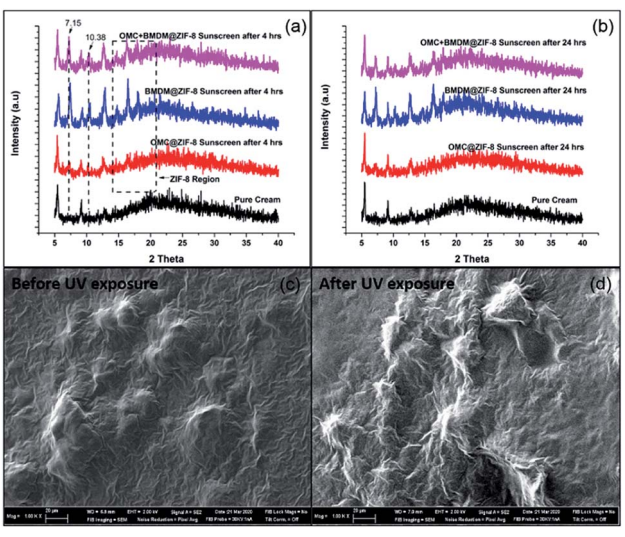

Fig. 5 Powder XRD patterns of OMC@ZIF-8, BMDM@ZIF-8, and OMC + BMDM@ZIF-8 nanocapsules after mixing with cream and UV exposure for (a) 4 h (b) 24 h and SEM images of OMC + BMDM@ZIF-8 sunscreen (c) before and (d) after UV exposure for 24 hours.

26.5, and 62.2 to 53.0, respectively, after 24 hours of UV irradiation as shown in Fig. 6(a). Prior reports indicated that the SPF value of sunscreen containing 10% OMC decreased from 20 to 13, and that of 10% BMDM decreased from 4 to 2 upon 12 hours of UV exposure.[16] SPF values of the sunscreens prepared here showed no significant decrease under UV radiation. The SPF of the OMC@ZIF-8 and BMDM@ZIF-8 sunscreen started increasing after 4 hours of UV radiation. Thus, these nanocapsules based sunscreens provide long-lasting sunscreen properties with ultra-high SPF.

The stability and retaining ability of microencapsulated ZIF-8 was assessed by measuring the release of UV filters in artificial sweat at 37 °C, as shown in Fig. 6(b). After 24 h, OMC@ZIF-8, BMDM@ZIF-8, and OMC + BMDM@ZIF-8 sunscreens released only 1.4%, 1.9%, and 1.0% of the total amount of UV filters present in them. The release amount of UV filters is almost negligible because of the nanoconfinement effect of ZIF-8. The small pores present in ZIF-8 offer high diffusion resistance to the leaching of UV filters from the ZIF-8. These results demonstrate that ZIF-8 could minimize the direct human skin contact risk of UV filters and provide excellent encapsulation stability. Therefore, these colorless nanocapsule-based sunscreens provide excellent photoprotection and good stability. This paper highlights the unique potential of effective and safe microencapsulated ZIF-8 based sunscreens for commercial development.

Experimental section

Materials and chemicals

Zinc acetate dihydrate (Fisher Scientific, Certified ACS), 2-methylimidazole (TCI Chemicals, >98%), OMC (Fisher Scientific), BMDM (Fisher Scientific), triethylamine (Fisher Scientific, 99%), syringe filters (Millipore Sigma), and Aveeno Daily Moisturizing Lotion for Dry Skin (CVS) were used as received.

Synthesis of ZIF-8 material nanocapsules

ZIF-8 nanocapsules were synthesized according to a reported method with some modifications.[18] Briefly, 100 mL ethanolic solution of 0.187 g of zinc acetate dihydrate was mixed with 100 mL ethanolic solution of 2-methylimidazole (0.738 g) under vigorous stirring with a magnetic stirrer. After 2 minutes, 100 μL of triethylamine was added to the above reaction mixture and stirring continued for 15 minutes at room temperature (25 °C). The clear solution slowly became turbid after about 5 minutes. After 15 minutes, the formed ZIF-8 nanocapsules were separated from the reaction mixture by centrifugation, followed by washing with ethanol. The solid was dried overnight at 50 °C.

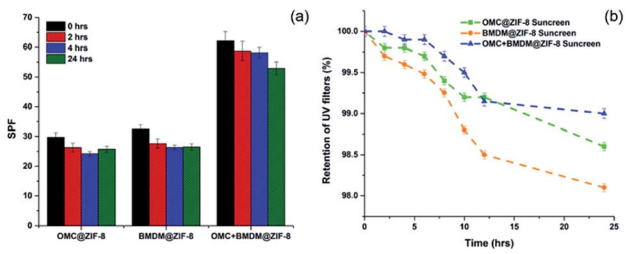

Fig. 6 Effect of (a) UV radiation on SPF values and (b) release study of OMC@ZIF-8, BMDM@ZIF-8, and OMC + BMDM@ZIF-8 nanocapsules after mixing with cream.

OMC@ZIF-8, BMDM@ZIF-8 and OMC + BMDM@ZIF-8 nanocapsules

Nanocapsules were produced by an *in situ* microencapsulation method. Briefly, a 100 mL ethanolic solution of 0.738 g of 2-methylimidazole was prepared, and 0.125 g of OMC (for OMC@ZIF-8) or BMDM (for BMDM@ZIF-8, with 100 μL of olive oil) or 0.0625 g each of OMC and BMDM (for OMC + BMDM@ZIF-8, with 100 μL of olive oil) was added into it. The reaction mixture was stirred well to obtain a clear and homogeneous solution. To the above solution, a 100 mL ethanolic solution of 0.187 g of zinc acetate dihydrate was mixed under vigorous stirring with a magnetic stirrer. After 2 minutes, 100 μL of triethylamine was added to the above reaction mixture and stirring continued for 15 minutes at room temperature (25 °C). The clear solution slowly became turbid after 5 minutes. After 15 minutes, the formed OMC@ZIF-8, BMDM@ZIF-8, or OMC + BMDM@ZIF-8 nanocapsules were separated from the reaction mixture by centrifugation, followed by washing with ethanol. The solid was dried overnight at 50 °C.

Encapsulation efficiency of OMC and BMDM in nanocapsules

To estimate the encapsulation efficiency of OMC and BMDM, the OMC@ZIF-8, BMDM@ZIF-8, and OMC + BMDM@ZIF-8 nanocapsules were collected by centrifugation at 10 000 rpm for 10 min. The amount of free UV-filters remaining in the supernatant was determined by UV-visible spectroscopy. The OMC and BMDM concentrations in the supernatant were calculated using calibration curves constructed from measurements on OMC and BMDM solutions of known concentration. The encapsulation efficiency was then calculated by subtracting the amount of free UV-filters in the supernatant from the total amount initially added during synthesis (Fig. S2†).

Stability of nanocapsules

The UV-vis spectrophotometery, XRD, and TEM determined the storage stability of the OMC@ZIF-8, BMDM@ZIF-8, and OMC + BMDM@ZIF-8 nanocapsules by recording their absorbance spectra, XRD spectra, and TEM images. The nanocapsules were dispersed in ethanol, kept in a dark chamber, and analysis was performed after 4 days, 7 days, 14 days, 28 days, and 40 days.

Preparation of nanocapsule-based sunscreens

The nanocapsule-based sunscreens were developed by blending the nanocapsules with Aveeno lotion. Briefly, 40 mg of each OMC@ZIF-8, BMDM@ZIF-8, and OMC + BMDM@ZIF-8 nanocapsules was mixed with 1 g of Aveeno lotion at 700 rpm for 20 minutes in a dark room. The prepared sunscreens were used for further studies.

Photostability and *in vitro* SPF assessment of nanocapsule-based sunscreens

For the evaluation of photostability, nanocapsule-based sunscreens and pure cream were uniformly spread onto plasma-cleaned microscope quartz glass slides using a 1 mL syringe. After drying for 10 minutes in a dark chamber, UV spectra, SEM, and XRD analysis of all four glass slides were performed before and after UV exposure. The UV spectra were recorded using a UV-vis spectrophotometer by measuring the absorbance (A) in the range of 290–400 nm. A blank quartz glass slide was used as a baseline. The photostability of all four samples was measured by monitoring the change in UV absorbance after UV exposure of 2, 4, and 24 h in a UV crosslinker chamber (UVP model CL1000, with five 8 W T5 bulbs, 365 nm).

The SPF of each sample was calculated by eqn (1).

$$\mathrm{SPF} = \frac{\sum_{400}^{290} E_\lambda S_\lambda}{\sum_{400}^{290} E_\lambda S_\lambda T_\lambda} \quad (1)$$

where E_λ = erythemal spectral effectiveness, S_λ = solar spectral irradiance, and T_λ = transmittance of the glass slide. The change in SPF of OMC@ZIF-8, BMDM@ZIF-8, and OMC + BMDM@ZIF-8 sunscreens was measured by irradiating the sunscreen-coated glass slides under UV crosslinker after 2 h, 4 h, and 24 h.

Evaluation of retention of OMC and BMDM in sunscreens

The ability of OMC@ZIF-8, BMDM@ZIF-8, and OMC + BMDM@ZIF-8 sunscreens to retain the UV filters was analyzed according to an established protocol with slight modifications.[7] Briefly, 10 mg of sunscreens were dispersed in 40 mL artificial sweat (0.5% NaCl, 0.1% urea, 0.1% lactic acid, and the pH adjusted to 6.6 with KOH) and kept on a magnetic stirrer for 24 h at 37 °C. At regular intervals of time, 200 μL of the solution was taken out, filtered with a 0.2 μm filter, and the same amount of fresh solution was added. The release of OMC and BMDM from the nanocapsule-based sunscreens was quantified by measuring the UV absorption of the filtered solution at 310 nm and 358 nm.

Material characterization

All UV absorption studies of free OMC, free BMDM, nanocapsules/sunscreens (OMC@ZIF-8, BMDM@ZIF-8, and OMC + BMDM@ZIF-8) were performed with a UV-vis spectrophotometer (Cary 7000) in the wavelength range of 200–600 nm or as described above.

The fluorescence spectra of free OMC, free BMDM, OMC@ZIF-8, BMDM@ZIF-8, and OMC + BMDM@ZIF-8 nanocapsules (1 mg mL^{-1} in ethanol) were recorded by exciting the samples at 228 nm using a Cary Eclipse spectrophotometer.

The size and morphology of ZIF-8, OMC@ZIF-8, BMDM@ZIF-8, and OMC + BMDM@ZIF-8 nanocapsules were characterized using a JEOL JEM 2010 Transmission Electron Microscope (TEM) operated at 200 kV. Dilute dispersions of samples were drop cast onto 200-mesh carbon-coated copper TEM grids obtained from Ted Pella.

The crystal structure of nanocapsules was determined by X-ray diffraction (XRD) analysis (Bruker Ultima IV with Cu Kα X-ray source) operated at 40 kV voltage and 44 mA current. All the XRD spectra were recorded at room temperature in the range of 5–40 degrees with a scan speed of 4 degrees min^{-1}.

Fourier Transform Infrared (FTIR) spectroscopy were recorded by measuring the transmittance of each sample in the range of 400–4000 cm^{-1} using a Bruker Vertex 70 spectrometer.

The morphology and structural stability analysis of sunscreen after UV exposure of 24 hours was performed using a cross-beam focused ion beam-scanning electron microscopy (FIB-SEM) (Carl Zeiss AURIGA). Before the examination, the samples were coated with an ultrathin layer of gold.

The surface area and pore size of nanocapsules were determined by N_2 physisorption measurements using a Micromeritics Tri-Star instrument. Before the measurement, all the samples were placed under vacuum overnight, followed by degassing using the degassing chamber at 150 °C for 4 hours. The pore size and specific surface area were calculated from Brunauer–Emmett–Teller (BET) adsorption–desorption data.

Conclusions

We demonstrate production of UV filter-loaded ZIF-8 nanocapsules with broad-spectrum UV protection, synthesized at room temperature within 15 minutes. The UV filter-loaded nanocapsules show enhanced UV-blocking ability compared to ZIF-8 or pure cream alone. The nanocapsules have excellent storage stability for over 40 days. Because of the photostabilization effect of nanocapsules, the SPF values of nanocapsule-loaded sunscreens were stable over 24 hours of UV exposure. The OMC + BMDM@ZIF-8 sunscreen shows a synergistic effect with high SPF (62) and excellent photostability (>85% retention of SPF after 24 hours UV exposure) compared to OMC@ZIF-8 and BMDM@ZIF-8 sunscreens. According to TEM images, the average size of nanocapsules was 200 nm, which would be sufficient to prevent penetration of nanocapsules into the skin. Microencapsulation of OMC and BMDM into microporous ZIF-8 not only prevents the release of these UV filters but also enhances their absorbance and minimizes the potential for direct skin exposure to these UV filters. Hence, these UV filter-loaded nanocapsules can be safe, cost-effective, biocompatible, and photostable, with excellent photoprotective performance.

Conflicts of interest

There are no conflicts to declare.

Acknowledgements

This present work was supported by the Indo-U.S. Overseas Fellowship for Women in STEMM (WISTEMM) from the Department of Science and Technology (DST), Government of

India. The authors also extend their thanks to Anita Yadav for her contributions.

References

1 N. D. N. Rodrigues, M. Staniforth and V. G. Stavros, *Proc. R. Soc. A*, 2016, **472**, 20160677.
2 D. R. Hayden, A. Imhof and K. P. Velikov, *ACS Appl. Mater. Interfaces*, 2016, **8**, 32655–32660.
3 H. Araki, J. Kim, S. Zhang, A. Banks, K. E. Crawford, X. Sheng, P. Gutruf, Y. Shi, R. M. Pielak and J. A. Rogers, *Adv. Funct. Mater.*, 2017, **27**, 1604465.
4 S. González, M. Fernández-Lorente and Y. Gilaberte-Calzada, *Clin. Dermatol.*, 2008, **26**, 614–626.
5 L. Chen, J. Y. Hu and S. Q. Wang, *J. Am. Acad. Dermatol.*, 2012, **67**, 1013–1024.
6 F. P. Gasparro, M. Mitchnick and J. F. Nash, *Photochem. Photobiol.*, 1998, **68**, 243–256.
7 L. Xu, D. Wu, B. Zhou, Y. Xu, W. Wang, D. Yu and D. Luo, *RSC Adv.*, 2018, **8**, 12315–12321.
8 I. Karlsson, L. Hillerström, A. L. Stenfeldt, J. Mårtensson and A. Börje, *Chem. Res. Toxicol.*, 2009, **22**, 1881–1892.
9 G. Vielhaber, S. Grether-Beck, O. Koch, W. Johncock and J. Krutmann, *Photochem. Photobiol. Sci.*, 2006, **5**, 275–282.
10 M. E. Balmer, H. R. Buser, M. D. Müller and T. Poiger, *Environ. Sci. Technol.*, 2005, **39**, 953–962.
11 L. A. MacManus-Spencer, M. L. Tse, J. L. Klein and A. E. Kracunas, *Environ. Sci. Technol.*, 2011, **45**, 3931–3937.
12 M. M. P. Tsui, J. C. W. Lam, T. Y. Ng, P. O. Ang, M. B. Murphy and P. K. S. Lam, *Environ. Sci. Technol.*, 2017, **51**, 4182–4190.
13 N. El-Haj and N. Goldstein, *Int. J. Dermatol.*, 2015, **54**, 362–366.
14 M. Schlumpf, K. Kypke, M. Wittassek, J. Angerer, H. Mascher, D. Mascher, C. Vökt, M. Birchler and W. Lichtensteiger, *Chemosphere*, 2010, **81**, 1171–1183.
15 H. V. Stein, C. J. Berg, J. N. Maung, L. E. O'Connor, A. E. Pagano, L. A. Macmanus-Spencer and M. G. Paulick, *Environ. Sci.: Processes Impacts*, 2017, **19**, 851–860.
16 X. Qiu, Y. Li, Y. Qian, J. Wang and S. Zhu, *ACS Appl. Bio Mater.*, 2018, **1**, 1276–1285.
17 H. Kaur, G. C. Mohanta, V. Gupta, D. Kukkar and S. Tyagi, *J. Drug Delivery Sci. Technol.*, 2017, **41**, 106–112.
18 S. K. Nune, P. K. Thallapally, A. Dohnalkova, C. Wang, J. Liu and G. J. Exarhos, *Chem. Commun.*, 2010, **46**, 4878–4880.
19 Y. Hu, H. Kazemian, S. Rohani, Y. Huang and Y. Song, *Chem. Commun.*, 2011, **47**, 12694–12696.
20 R. Su, W. Fan, Q. Yu, X. Dong, J. Qi, Q. Zhu, W. Zhao, W. Wu, Z. Chen, Y. Li and Y. Lu, *Oncotarget*, 2017, **8**, 38214–38226.

